

# LECTURE NOTES IN PHYSICS

G. Contopoulos  
N. Voglis  
(Eds.)

## Galaxies and Chaos



Springer



## LECTURE NOTES IN PHYSICS

Contopoulos · Voglis (Eds.)

### Galaxies and Chaos

In this book the application of tools developed for Nonlinear Dynamical Systems to Galactic Dynamics and Galaxy Formation, as well as to related issues in Celestial Mechanics, is examined. The contributions collected in this book have emerged from selected presentations at a workshop on this topic and have been suitably expanded in order to be accessible to nonspecialist researchers and postgraduate students wishing to enter this exciting field of research.

ISSN 0075-8450

ISBN 3-540-40470-8



<http://www.springer.de>

*Available  
online*  
[www.springerlink.com/series/lnp/](http://www.springerlink.com/series/lnp/)



# Collisionless Evaporation from Cluster Elliptical Galaxies

Veruska Muccione<sup>1</sup> and Luca Ciotti<sup>2</sup>

<sup>1</sup> Geneva Observatory, 51. ch. des Maillettes, 1290 Sauverny, Switzerland

<sup>2</sup> Dipartimento di Astronomia, Università di Bologna, via Ranzani 1, 40127 Bologna, Italy

**Abstract.** We describe a particular aspect of the effects of the parent cluster tidal field (CTF) on stellar orbits inside cluster Elliptical galaxies (Es). In particular we discuss, with the aid of a simple numerical model, the possibility that *collisionless stellar evaporation* from elliptical galaxies is an effective mechanism for the production of the recently discovered intracluster stellar populations (ISP). A preliminary investigation, based on very idealized galaxy density profiles (Ferrers density distributions), showed that over an Hubble time, the amount of stars lost by a representative galaxy may sum up to the 10% of the initial galaxy mass, a fraction in interesting agreement with observational data. The effectiveness of this mechanism is due to the fact that the galaxy oscillation periods near equilibrium configurations in the CTF are comparable to stellar orbital times in the external galaxy regions. Here we extend our previous study to more realistic galaxy density profiles, in particular by adopting a triaxial Hernquist model.

## 1 Introduction

Observational evidences of an Intracluster Stellar Population (ISP) are mainly based on the identification of *intergalactic* planetary nebulae and red giant stars (see, e.g., [1],[2],[3],[4],[5]). Overall, the data suggest that approximately 10% (or even more) of the stellar mass of clusters is contributed by the ISP [6]. The usual scenario assumed to explain the finding above is that gravitational interactions between cluster galaxies, and interactions between the galaxies with the gravitational field of the cluster, lead to a substantial stripping of stars from the galaxies themselves.

Here, supported by a curious coincidence, namely by the fact that *the characteristic times of oscillation of a galaxy around its equilibrium position in the cluster tidal field (CTF) are of the same order of magnitude of the stellar orbital periods in the external part of the galaxy itself*, we explore the effects of interaction between stellar orbits inside the galaxies and the CTF. In fact, based on the observational evidence that the major axis of cluster Es seems to be preferentially oriented toward the cluster center, N-body simulations showed that model galaxies tend to align, as observed, reacting to the CTF as rigid bodies [7]. By assuming this idealized scenario, a stability analysis then showed that this configuration is of stable equilibrium, and allowed to calculate the oscillation periods in the linearized regime [8]. In particular, oscillations around two stable equilibrium configurations have been considered, namely: 1) when the center

of mass of the galaxy is at rest at center of a triaxial cluster, and the galaxy inertia ellipsoid is aligned with the CTF principal directions, and 2) when the galaxy center of mass is placed on a circular orbit in a spherical cluster, and the galaxy major axis points toward the galaxy center while the galaxy minor axis is perpendicular to the orbital plane.

Here, prompted by these observational and theoretical considerations, we extend a very preliminary study of the problem [9], by evolving stellar orbits in a more realistic galaxy density profile: for simplicity we restrict to case 1) above, while the full exploration of the parameter space, together with a complete discussion of case 2), will be given elsewhere [10]. It is clear, however, that both cases are rather exceptional. Most cluster galaxies neither rest in the cluster center nor move on circular orbits, but they move on elongated orbits with very different pericentric and apocentric distances from the cluster's center; in a triaxial cluster many orbits are boxes and some orbits can be chaotic. These latter cases can be properly investigated only by direct numerical simulation of the stellar motions inside the galaxies, coupled with the numerical integration of the equations of the motion of the galaxies themselves.

## 2 The Physical Background

Without loss of generality we assume that in the (inertial) Cartesian coordinate system  $C$ , with the origin on the cluster center, the CTF tensor  $\mathbf{T}$  is in diagonal form, with components  $T_i$  ( $i = 1, 2, 3$ ). By using three successive, counterclockwise rotations ( $\varphi$  around  $x$  axis,  $\vartheta$  around  $y'$  axis and  $\psi$  around  $z''$  axis), the linearized equations of the motion for the galaxy near the equilibrium configuration can be written as

$$\ddot{\varphi} = \frac{\Delta T_{32} \Delta I_{32}}{I_1} \varphi, \quad \ddot{\vartheta} = \frac{\Delta T_{31} \Delta I_{31}}{I_2} \vartheta, \quad \ddot{\psi} = \frac{\Delta T_{21} \Delta I_{21}}{I_3} \psi, \quad (1)$$

where  $\Delta T$  is the antisymmetric tensor of components  $\Delta T_{ij} \equiv T_i - T_j$ , and  $I_i$  are the principal components of the galaxy inertia tensor. In addition, let us also assume that  $T_1 \geq T_2 \geq T_3$  and  $I_1 \leq I_2 \leq I_3$ , i.e., that  $\Delta T_{32}, \Delta T_{31}$  and  $\Delta T_{21}$  are all less or equal to zero (see, e.g., [8], [10]). Thus, the equilibrium position associated with (1) is *linearly stable*, and its solution is

$$\varphi = \varphi_M \cos(\omega_\varphi t), \quad \vartheta = \vartheta_M \cos(\omega_\vartheta t), \quad \psi = \psi_M \cos(\omega_\psi t), \quad (2)$$

where

$$\omega_\varphi = \sqrt{\frac{\Delta T_{23} \Delta I_{32}}{I_1}}, \quad \omega_\vartheta = \sqrt{\frac{\Delta T_{13} \Delta I_{31}}{I_2}}, \quad \omega_\psi = \sqrt{\frac{\Delta T_{12} \Delta I_{21}}{I_3}}. \quad (3)$$

For computational reasons the best reference system in which calculate stellar orbits is the (non inertial) reference system  $C'$  in which the galaxy is at rest, and its inertia tensor is in diagonal form. The equation of the motion for a star in  $C'$  is

$$\ddot{\mathbf{x}}' = \mathcal{R}^T \ddot{\mathbf{x}} - 2\boldsymbol{\Omega} \wedge \mathbf{v}' - \dot{\boldsymbol{\Omega}} \wedge \mathbf{x}' - \boldsymbol{\Omega} \wedge (\boldsymbol{\Omega} \wedge \mathbf{x}'), \quad (4)$$



where  $\mathbf{x} = \mathcal{R}(\varphi, \vartheta, \psi)\mathbf{x}'$ , and

$$\boldsymbol{\Omega} = (\dot{\varphi} \cos \vartheta \cos \psi + \dot{\vartheta} \sin \psi, -\dot{\varphi} \cos \vartheta \sin \psi + \dot{\vartheta} \cos \psi, \dot{\varphi} \sin \vartheta + \dot{\psi}). \quad (5)$$

In (4)

$$\mathcal{R}^T \ddot{\mathbf{x}} = -\nabla_{\mathbf{x}'} \phi_g + (\mathcal{R}^T \mathbf{T} \mathcal{R}) \mathbf{x}', \quad (6)$$

where  $\phi_g(\mathbf{x}')$  is the galactic gravitational potential,  $\nabla_{\mathbf{x}'}$  is the gradient operator in  $C'$ , and we used the tidal approximation to obtain the star acceleration due to the cluster gravitational field.

### 3 Galaxy and Cluster Models

For simplicity we assume that the galaxy and cluster densities are stratified on homeoids. In particular, the galaxy density belongs to ellipsoidal generalization of the widely used  $\gamma$ -models ([11],[12]):

$$\rho_g(m) = \frac{M_g}{\alpha_1 \alpha_2 \alpha_3} \frac{3 - \gamma}{4\pi} \frac{1}{m^\gamma (1 + m)^{4 - \gamma}}, \quad (7)$$

where  $M_g$  is the total mass of the galaxy,  $0 \leq \gamma \leq 3$  and

$$m^2 = \sum_{i=1}^3 \frac{(x'_i)^2}{\alpha_i^2}, \quad \alpha_1 \geq \alpha_2 \geq \alpha_3. \quad (8)$$

The inertia tensor components of a generic homeoidal density distribution (in the natural reference system adopted in (8)), are given by

$$I_i = \frac{4\pi}{3} \alpha_1 \alpha_2 \alpha_3 (\alpha_j^2 + \alpha_k^2) h_g, \quad (9)$$

where  $h_g = \int_0^\infty \rho_g(m) m^4 dm$ , and so  $I_1 \leq I_2 \leq I_3$ . Note that, from (3) and (9) it results that the frequencies for homeoidal stratifications *do not depend on the specific density distribution assumed*, but only on the quantities  $(\alpha_1, \alpha_2, \alpha_3)$ . We also introduce the two ellipticities

$$\frac{\alpha_2}{\alpha_1} \equiv 1 - \epsilon, \quad \frac{\alpha_3}{\alpha_1} \equiv 1 - \eta, \quad (10)$$

where  $\epsilon \leq \eta \leq 0.7$ .

A rough estimate of *characteristic stellar orbital times* inside  $m$  is given by  $P_{orb}(m) \simeq 4P_{dyn}(m) = \sqrt{3\pi/G\bar{\rho}_g(m)}$ , where  $\bar{\rho}_g(m)$  is the mean galaxy density inside  $m$ . We thus obtain

$$P_{orb}(m) \simeq 9.35 \times 10^6 \sqrt{\frac{\alpha_{1,1}^3 (1 - \epsilon)(1 - \eta)}{M_{g,11}}} m^{\gamma/2} (1 + m)^{(3 - \gamma)/2} \text{ yrs}, \quad (11)$$

where  $M_{g,11}$  is the galaxy mass normalized to  $10^{11} M_\odot$ ,  $\alpha_{1,1}$  is the galaxy “core” major axis in kpc units (for the spherically symmetric  $\gamma = 1$  Hernquist model [13],



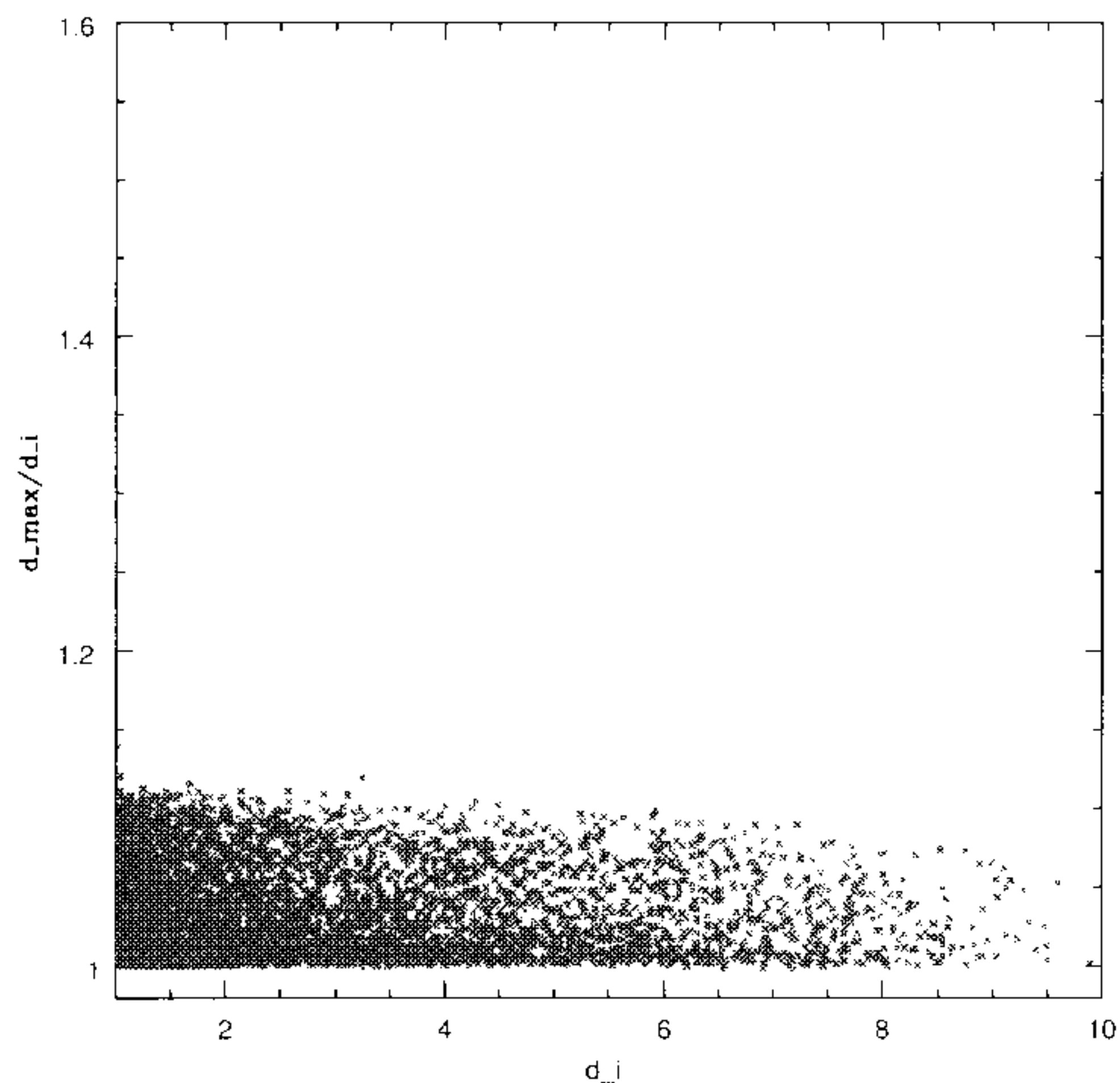


**Fig. 1.** Distribution of the  $d_{\max}/d_i$  ratio vs.  $d_i/\alpha_1$  after an Hubble time for the model galaxy at rest.  $d_i$  is the initial distance of the star from the galaxy center, while  $d_{\max}$  is the maximum distance from the galaxy center reached during the simulation.

$R_c \simeq 1.8\alpha_1$ ); thus, in the outskirts of normal galaxies orbital times well exceed  $10^8$  or even  $10^9$  yrs. For the cluster density profile we assume

$$\rho_c(m) = \frac{\rho_{c,0}}{(1 + m^2)^2}, \quad (12)$$

where  $m$  is given by an identity similar to (8), with  $a_1 \geq a_2 \geq a_3$ , and, in analogy with (10) we define  $a_2/a_1 \equiv 1 - \mu$  and  $a_3/a_1 \equiv 1 - \nu$ , with  $\mu \leq \nu \leq 1$ . It can be shown (see, e.g., [8],[10]) that the CTF components at the center of a non-singular homeoidal distribution are given by

$$T_i = -2\pi G \rho_{c,0} w_i(\mu, \nu), \quad (13)$$

where the dimensionless quantities  $w_i$  are independent of the specific density profile,  $w_1 \leq w_2 \leq w_3$  for  $a_1 \geq a_2 \geq a_3$ , and so the conditions for stable equilibrium in (1) are fulfilled ([8],[10]). The quantity  $\rho_{c,0}$  is not a well measured quantity in real clusters, and for its determination we use the virial theorem,  $M_c \sigma_V^2 = -U$ , where  $\sigma_V^2$  is the virial velocity dispersion, that we assume to be estimated by the observed velocity dispersion of galaxies in the cluster. Thus, we can now compare the galactic oscillation periods:

$$\begin{aligned} P_\varphi &= \frac{2\pi}{\omega_\varphi} \simeq \frac{8.58 \times 10^8}{\sqrt{(\nu - \mu)(\eta - \varepsilon)}} \frac{a_{1,250}}{\sigma_{V,1000}} \text{ yrs} , \\ P_\vartheta &= \frac{2\pi}{\omega_\vartheta} \simeq \frac{8.58 \times 10^8}{\sqrt{\nu\eta}} \frac{a_{1,250}}{\sigma_{V,1000}} \text{ yrs} , \\ P_\psi &= \frac{2\pi}{\omega_\psi} \simeq \frac{8.58 \times 10^8}{\sqrt{\mu\varepsilon}} \frac{a_{1,250}}{\sigma_{V,1000}} \text{ yrs} . \end{aligned}$$



(for small galaxy and cluster flattenings, where  $a_{1,250} = a_1/250$  kpc and  $\sigma_{V,1000} = \sigma_V/10^3$  km/s, [10]) with the characteristic orbital times in galaxies. Thus, from (11) and (14abc), it follows that *in the outer halo of giant Es, stellar orbital times can be of the same order of magnitude as the oscillatory periods of the galaxies themselves near their equilibrium position in the CTF*. For example, in a relatively small galaxy of  $M_{g,11} = 0.1$  and  $\alpha_{1,1} = 1$ ,  $P_{orb} \simeq 1$  Gyr at  $m \simeq 10$  (i.e., at  $\simeq 5R_e$ ), while for a galaxy with  $M_{g,11} = 1$  and  $\alpha_{1,1} = 3$  the same orbital time characterizes  $m \simeq 7$  (i.e.,  $\simeq 3.5R_e$ ).

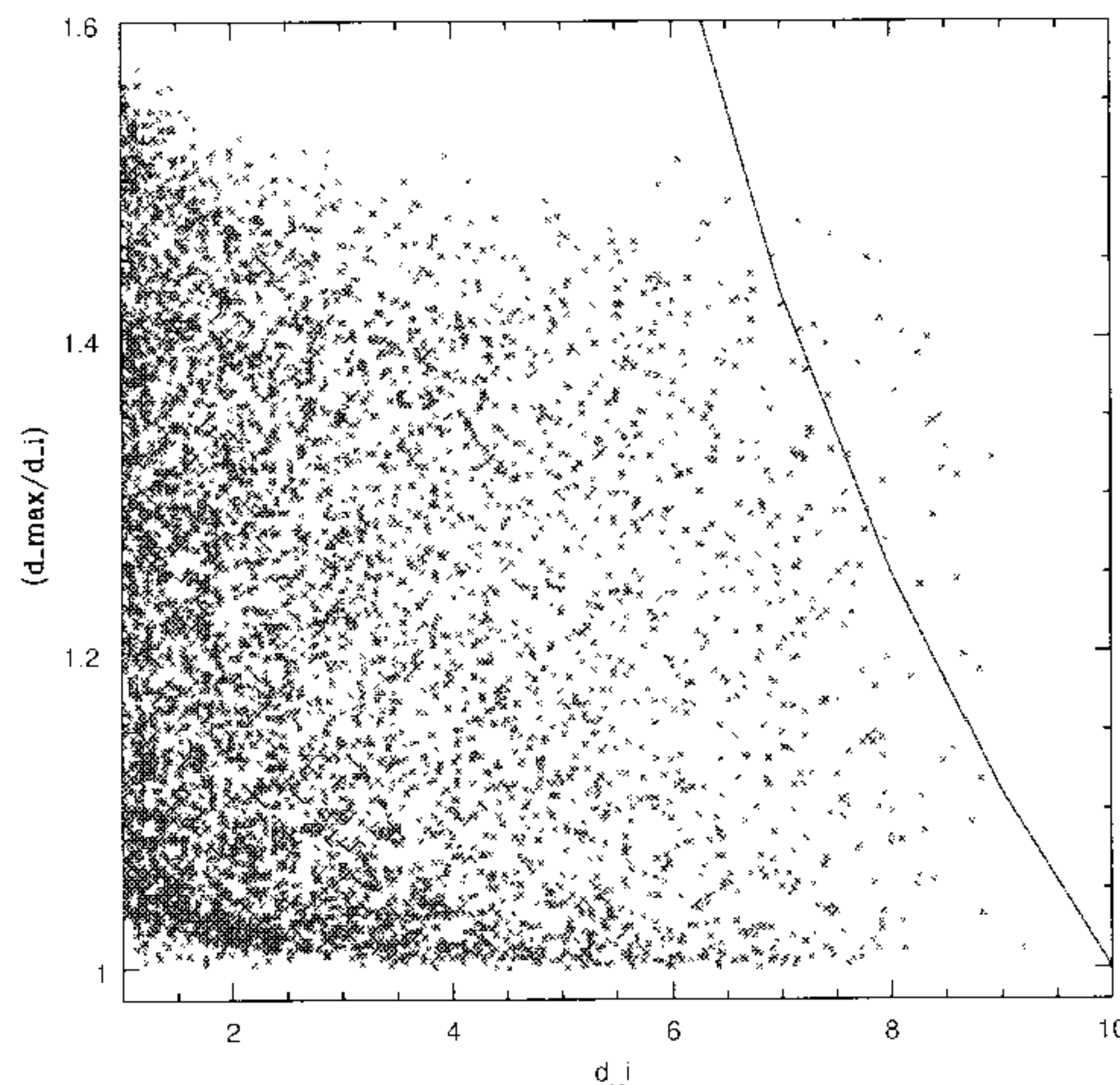


**Fig. 2.** Distribution of the  $d_{\max}/d_i$  ratio vs.  $d_i/\alpha_1$  after an Hubble time for the same galaxy model as in Fig. 1, when oscillating around its equilibrium position in the CTF.

In order to understand the effects of the galaxy oscillations on the stellar orbits, we performed a set of Monte-Carlo simulations, in which we followed the evolution of  $10^4 - 10^5$  “1-body problems” over the Hubble time by integrating numerically (4). At variance with [9], where we used simple and easy-to-integrate Ferrers density profiles, here we study orbital evolution in a more realistic (but also more demanding from the numerical point of view) galaxy density profile, namely a triaxial Hernquist model, obtained by assuming  $\gamma = 1$  in (7). The gravitational potential inside the galaxy density distribution, in a form suitable for the numerical integration, was obtained by using an expansion technique useful in case of small density flattenings ([10],[14]). The initial conditions are generated by using the Von Neumann rejection method in phase-space (for details see [10]): note that, at variance with the analysis [9], now “stars” are characterized by initial velocities that can be different from zero. The code, a double-precision fortran code based on a Runge-Kutta scheme, runs on GRAVITOR, the Geneva Observatory 132 processors Beowulf cluster ([http://obswww.unige.ch/~pfennige/gravitor/gravitor\\_e.html](http://obswww.unige.ch/~pfennige/gravitor/gravitor_e.html)). The computation of  $10^4$  orbits usually requires 2 hours when using 10 nodes.



## 4 Preliminary Results and Conclusions

We show here, as an illustrative case, the behavior of the ratio  $d_{\max}/d_i$  as a function of  $d_i/\alpha_1$ , for a moderately flattened galaxy model ( $\epsilon \simeq 0.2$  and  $\eta \simeq 0.3$ ), with  $M_g = 10^{11} M_\odot$ , semi-major axis  $\alpha_1 = 3$  kpc, and maximum oscillation angles equals to 0.1 rad. The cluster parameters are  $a_{1,250} = \sigma_{V,1000} = 1$ ,  $\mu = 0.2$ ,  $\nu = 0.4$ , and the total number of explored orbits is  $N_{\text{tot}} = 10^4$ . In order to show the effect of oscillations, in the following simulations we artificially eliminated the *direct* contribution of the CTF, as given by the second term in the r.h.s. of (6).

In Fig. 1 we show the result of a first simulation in which the galaxy is *not* oscillating: obviously, the ratio  $d_{\max}/d_i$  is in general (slightly) larger than unity, due to the initial velocity of each star. In Fig. 2 we show the result for the same galaxy model, when oscillating around the equilibrium position: the effects of the galaxy oscillations are clearly visible as a global “expansion” of the galaxy. As a reference, the solid line indicates the expansion ratio required to reach the representative distance of  $10R_e$  from the galaxy center. Thus, it is clear that the galaxy oscillations are certainly able to substantially modify the galaxy density profile. In particular, it will be of interest the study of the (more realistic) case in which the galaxy is in rotation around the cluster center. In this case we expect a different behavior of stellar orbits as a function of the distance of the galaxy center of mass from the cluster center: in fact, while inside the cluster core the CTF is *compressive* (see, e.g., [7],[8]), outside the CTF is *expansive* along the cluster radial direction, and in this latter case its direct effect should increase the expansive effect due to the galaxy oscillations. These cases are discussed in detail in [10].

## References

1. T.Theuns, S.J. Warren: MNRAS, 284 (1996)
2. R.H. Méndez et al: ApJ, 491 (1998)
3. J.J. Feldmeier , R. Ciardullo, G.H. Jacoby: ApJ, 503 (1998)
4. M. Arnaboldi, J.A.L. Aguerri, N.R. Napolitano, O. Gerhard, K.C. Freeman, J. Feldmeier , M. Capaccioli, R.P. Kudritzki, R.H. Méndez: AJ, 123 (2002)
5. P.R. Durrell, R. Ciardullo, J.J. Feldmeier, G.H. Jacoby, S. Sigurdsson: ApJ, 570 (2002)
6. H.C. Ferguson, N.R. Tanvir, T. von Hippel: Nature, 391 (1998)
7. L. Ciotti, S.N. Dutta: MNRAS, 270 (1994)
8. L. Ciotti, G. Giampieri: Cel. Mech. & Dyn. Astr., 68 (1998)
9. V. Muccione, L. Ciotti: Mem. S.A.It., in press (2003)
10. L. Ciotti, V. Muccione: in preparation
11. W. Dehnen: MNRAS, 256 (1993)
12. S. Tremaine et al.: AJ, 107 (1994)
13. L. Hernquist: ApJ, 356, 359 (1990)
14. L. Ciotti, G. Bertin: in preparation